

# B7-H3 Regulates Glioma Growth and Cell Invasion Through a JAK2/STAT3/Slug-Dependent Signaling Pathway

This article was published in the following Dove Press journal:  
*OncoTargets and Therapy*

Chuanhong Zhong<sup>1,2</sup>

Bei Tao<sup>3</sup>

Yitian Chen<sup>4</sup>

Zhangchao Guo<sup>1</sup>

Xiaobo Yang<sup>1,2</sup>

Lilei Peng<sup>1,2</sup>

Xiangguo Xia<sup>1,2</sup>

Ligang Chen<sup>1,2</sup>

<sup>1</sup>Neurosurgery Department, Affiliated Hospital of Southwest Medical University, Luzhou, People's Republic of China;

<sup>2</sup>Neurosurgical Clinical Medical Research Center of Sichuan Province, Luzhou, People's Republic of China; <sup>3</sup>Rheumatism Department, Affiliated Hospital of Southwest Medical University, Luzhou, People's Republic of China; <sup>4</sup>Department of Clinical Medicine, Medical College of Soochow University, Suzhou, People's Republic of China

**Purpose:** The aim of this study was to explore the potential role of B7-H3 in malignant glioma progression and identify an innovative approach in clinical glioma therapy.

**Methods:** The protein expression of B7-H3 in high- and low-grade tumor tissues from glioma patients was assessed by immunohistochemistry. The proliferative and invasive ability of B7-H3-overexpressing or knockout glioma cells was analyzed in vitro and in vivo by CCK-8 assay and an orthotopic mouse glioma model, respectively. Activation of the JAK2/STAT3/Slug signaling pathway and epithelial–mesenchymal transition (EMT) was examined by Western blotting and immunofluorescence. The anticancer effects of napabucasin (NAP) and temozolomide (TMZ) were analyzed in an orthotopic mouse glioma model.

**Results:** The expression of B7-H3 was higher in high-grade than in low-grade tumor tissues from glioma patients. In line with this, overexpression of B7-H3 enhanced glioma cell proliferation, induced sustained glioma growth, and promoted glioma cell invasion in vitro and in vivo. Moreover, these effects were mediated through the activation of the JAK2/STAT3/Slug signaling pathway in B7-H3 overexpression glioma cells. We also found that B7-H3 induced EMT processes through downregulation of E-cadherin and upregulation of MMP-2/-9 expression, resulting in enhanced invasion of glioma cells. Finally, we show that the combination of NAP and TMZ significantly suppressed glioma growth and glioma cell invasion, both in vitro and in vivo.

**Conclusion:** B7-H3 overexpression facilitated sustained glioma growth and promoted glioma cell invasion through a JAK2/STAT3/Slug-dependent signaling pathway. Application of the STAT3 inhibitor NAP significantly suppressed glioma growth and invasion, and has potential as a therapeutic strategy for the treatment of glioma.

**Keywords:** B7-H3, glioma, JAK2/STAT3/Slug, temozolomide

## Introduction

Glioma accounts for approximately half of all primary malignant brain carcinomas, and exhibits a highly aggressive phenotype and high incidence rate worldwide.<sup>1,2</sup> Despite sustained efforts to treat glioma, including maximal surgery, adjuvant radiation, and chemotherapy, the median survival remains poor (12–16 months) and the 5-year survival rate is less than 10% in patients with malignant glioma.<sup>3,4</sup> Several factors are believed to be crucial for the poor outcomes associated with glioma patients, including an invasive tumor microenvironment, acquired multidrug resistance, and sustained tumor growth induced by pro-survival signaling pathways.<sup>5</sup> Consequently,

Correspondence: Ligang Chen  
Neurosurgery Department, Affiliated Hospital of Southwest Medical University, Luzhou 646000, People's Republic of China  
Tel/Fax +86 181 13556657  
Email chenligang199066@163.com

innovative approaches are urgently needed to suppress glioma growth and invasion for improved glioma treatment.

B7-H3 (CD276), which in humans is composed of a 2Ig- and a 4Ig-B7H3 isoform, is a well-characterized checkpoint molecule in immune cells. Enhanced expression of B7-H3 can suppress type I interferon-gamma expression in T cells and reduce the cytotoxic killing effects exerted by natural killer (NK) cells.<sup>6,7</sup> B7-H3 is also known to exert costimulatory and coinhibitory effects in T cell responses.<sup>6,8</sup> Increasing evidence has indicated that the B7-H3 protein is highly expressed in several tumor types, including gastric, liver, colorectal, and prostate cancers.<sup>9–12</sup> Elevated expression of B7-H3 has been shown to lead to increased tumor grade, distant cancer metastasis, acquired drug resistance, and poor overall survival in glioma patients.<sup>13,14</sup> However, whether B7-H3 has a role in glioma development remains unclear.

Several studies have indicated that B7-H3 can activate prosurvival signaling pathways in tumor cells, resulting in sustained tumor growth and progression.<sup>15,16</sup> The JAK/STAT3 signal, which is associated with somatic cell proliferation and differentiation, has been detected in various tumor cells and is known to promote tumor progression.<sup>17–19</sup> Activation of JAK/STAT3 signaling can directly regulate tumor growth and promote EMT processes, resulting in the invasion and metastasis of gastric and ovarian cancer cells.<sup>20,21</sup> Notably, B7-H3 can upregulate the expression of JAK/STAT3 to facilitate the distant metastasis of myeloma cells, suggesting that JAK/STAT3 signaling may have a role in B7-H3-induced tumor progression.<sup>22</sup>

In our study, we observed that B7-H3 was highly expressed in malignant glioma tissues. Importantly, we found that enhanced B7-H3 expression could significantly promote glioma cell proliferation and invasion both *in vitro* and *in vivo*, resulting in poor clinical prognosis. Expression of B7-H3 in glioma could activate the JAK2/STAT3 prosurvival signaling pathway, resulting in tumor growth and induction of EMT in cancer cells. Additionally, glioma cells overexpressing B7-H3 showed elevated expression of MMP-2 and MMP-9 and downregulation of the levels of the adhesion molecule E-cadherin, thereby providing a possible explanation for the mechanisms underlying glioma invasion. Based on these results, we combined the STAT3 inhibitor NAP with the chemotherapeutic agent TMZ to treat mice in an orthotopic glioma model. This combination treatment exerted a significant antiglioma effect, thereby providing a novel and innovative approach for the treatment of this tumor.

## Materials and Methods

### Cell Culture and Reagents

LN229 and U87 cells were obtained from the Cell Bank of the Chinese Academy of Sciences (Shanghai, China) and cultured in DMEM (Gibco, MA, USA) supplemented with 10% fetal bovine serum (FBS) (Gibco) and antibiotics (50 U/mL penicillin and 100 µg/mL streptomycin; Gibco) at 37 °C in 5% CO<sub>2</sub>. Napabucasin (NAP) and FLLL32 were obtained from Selleck Chemicals (Houston, TX, USA). Temozolomide (TMZ) and paraformaldehyde were purchased from Sigma–Aldrich (MA, USA). D-luciferin and crystal violet were purchased from Beyotime (Shanghai, China). The human MMP2 and MMP9 Elisa Kits were purchased from Abcam (Cambridge, UK).

### Tumor Tissue Collection and Ethic Statement

Tissues from glioma patients were collected from excess surgical resection samples at the Affiliated Hospital of Southwest Medical University. Glioma had been diagnosed by neuropathology with the necessary consent and in accordance with an IRB-approved protocol (IRB number: k2018010). Sample collection and processing were performed according to the Declaration of Helsinki. All patients provided signed and informed consent before tumor tissue collection and tissue treatment, including for the use of their data for further research. All experiments were carried out under the supervision of the Ethics Committee of the Affiliated Hospital of Southwest Medical University. Samples were collected and sent to the laboratory within 2 h for clinicopathological analysis. The samples were divided into high-grade and low-grade groups based on the clinical data and WHO classification guidelines (high-grade gliomas: WHO level 3–4; low-grade gliomas: WHO level 1–2).

### Cell Proliferation and Colony Formation Assays

For the cell proliferation assay,  $5 \times 10^3$  cells were seeded into 96-well plates in triplicate, and a Cell Counting Kit-8 (CCK-8) (Dojindo, Kumamoto, Japan) was used to monitor the cell proliferation rate continuously for 72 h. For the colony formation assay, 500 cells were seeded into 6-well plates at 37 °C in a humidified incubator. After 14 days, the cells were fixed in 4% paraformaldehyde and then stained with 0.05% crystal violet. Colonies (>50 cells) were subsequently counted manually.

## Plasmid Constructs, Lentivirus Production, and Cell Transduction

The coding sequences of human B7-H3 and luciferase were amplified and cloned into the pLVX-IRES-Puro vector from GenePharma (Shanghai, China). To establish stable B7-H3 knockout cells, three lentiCRISPR-Cas9-sgRNA-hB7H3 vectors and the control lentiCRISPR-Cas9 vector were obtained from GenePharma. Lentivirus was produced by GenePharma and infected glioma cells. After 96 h, the cells were screened by puromycin selection. The anti-human Slug siRNA was purchased from Ribobio (Guangzhou, China) and transfected into glioma cells using Lipo8000 (Beyotime, China). The Slug siRNA sequence was 5'-UCCGAAUAUGCAUCUUCAGG GCGCCCA-3' and that of the negative control was 5'-UCAC AAGGGAGAGAAAGAGAGGAAGGA-3'. Overexpression and knockout efficiency were determined by Western blotting.

## Transwell Assay

For the migration assay, LN229 and U87 cells ( $1 \times 10^4$  cells) were seeded into the upper transwell chamber (8  $\mu$ m, Corning Inc. USA). The bottom chamber was filled with 0.5 mL of medium containing 20% FBS. After 24 h, the cells were fixed in 4% paraformaldehyde and then stained with 0.05% crystal violet. The number of tumor cells that penetrated the membrane was counted in six random fields.

## Western Blotting

Cell lysates were separated by SDS-PAGE, transferred onto nitrocellulose membranes, and immunoblotted with the following antibodies: anti- $\beta$ -actin (Santa Cruz Biotechnology, CA, USA), anti-CD276, anti-STAT3 (phospho S727), anti-STAT3, anti-JAK2 (phospho Y1007+Y1008), anti-JAK2, anti-SOCS-3, anti-SHP1, anti-SHP1 (phospho Y536), anti-Src, anti-Src (phospho Y529), anti-E-Cadherin, anti-N-Cadherin, and anti-Slug (all from Abcam).

## Immunofluorescence

Cells were fixed in 4% formaldehyde for 10 min, permeabilized with 0.2% Triton X-100, and blocked with goat serum for 30 min at room temperature. The cells were incubated with anti-STAT3 (phospho S727) (1:100, Abcam), anti-JAK2 (phospho Y1007+Y1008) (1:100, Abcam), or anti-Slug antibodies (1:100, Abcam) overnight at 4°C. The next day, the samples were incubated with secondary antibody for 60 min at room temperature and the nuclei were counterstained with 4',6-diamidino-2-phenylindole (DAPI) (Beyotime) at room temperature for 3 min. Images were

acquired using a confocal microscope (Olympus, Tokyo, Japan).

## Bioinformatic Analysis

A normalized mRNA expression dataset for glioblastoma multiforme was downloaded from the GEPIA server (<http://gepia.cancer-pku.cn/>) for cancer genomics and used to evaluate the expression of CD276/B7-H3 transcripts in brain lower-grade glioma (LGG) (The Cancer Genome Atlas, TCGA). This dataset includes mRNA profiles for 514 brain LGG cases and overall survival analysis was calculated for these transcripts.

## In vivo Animal Experiments

All animal protocols in our experiments were conducted in accordance with the Southwest Medical University animal welfare guidelines and approved by the Institutional Animal Care and Use Committee of the Affiliated Hospital of Southwest Medical University. For tumorigenesis analysis, male nude mice (6–8 weeks old) were purchased from the Beijing HFK company (Beijing, China). The animals were randomly assigned to groups ( $n = 10$ /group) and subcutaneously inoculated in the right flank with  $5 \times 10^4$  cells. Tumor numbers were counted 30 days after injection. For the orthotopic tumor model, male nude mice (6–8 weeks old) were intracranially injected with  $1 \times 10^6$  luciferase-marked glioma cells using a mouse stereotaxic instrument (Stoelting, CA, USA). Mice were randomly divided into 4 groups after 2 weeks ( $n = 5$  per group). On day 20, the mice were orally administered PBS, NAP (5 mg/kg), TMZ (10 mg/kg), or TMZ (10 mg/kg) plus NAP (5 mg/kg) twice a week. Treatment was performed for 2 weeks. Isoflurane was used for anesthesia. Mice were imaged for 10 min after intraperitoneal injection of D-luciferin (250 mg/kg) for bioluminescence. The signal intensity of tumor cells was quantified within a head region using Living Image software (PerkinElmer, MA, USA).

## Results

### B7-H3 Expression Promoted Glioma Growth and Glioma Cell Invasion

A recent study showed that B7-H3 expression is strictly correlated with malignant neoplastic progression in several tumor types.<sup>23</sup> To investigate the potential role of B7-H3 in glioma development, we collected tumor tissues from glioma patients and examined the expression profile of B7-H3 by immunohistochemistry. Expression of B7-H3 was higher in high-grade

glioma tissues (H-M, WHO grade 3–4) than in low-grade glioma tissue (L-M, WHO grade 1–2) (Figure 1A). This pattern was observed in multiple patients in the H-M glioma group (Figure 1B,  $n = 10$ ), indicating that B7-H3 might be involved in glioma progression. To further elucidate the mechanism underlying B7-H3-induced glioma development, we generated B7-H3 overexpression or knockout LN229 glioma cells (LN229-B7-H3 OE and LN229-B7-H3 KO, respectively) and U87 glioma cells (U87-B7-H3 OE and U87-B7-H3 KO, respectively) (Figure 1C). Notably, overexpression of B7-H3 significantly enhanced the proliferative capacity of glioma cells and sustained tumor growth in vitro and in vivo, whereas B7-H3 knockout suppressed these effects (Figure 1D and E). B7-H3 expression also increased colony formation and tumorigenesis in LN229 and U87 cells (Figure 1F and G), indicating that B7-H3 could efficiently facilitate proliferation and tumorigenesis in glioma cells. Importantly, proliferative glioma cells exhibited enhanced stem-like phenotypes, as well as highly invasive properties, in malignant glioma patients. Overexpression of B7-H3 also enhanced the invasive ability of LN229 and U87 cells, whereas blockade of B7-H3 strongly suppressed this effect (Figure 1H), suggesting that B7-H3 has a crucial role in glioma cell invasion. Kaplan–Meier analysis of TCGA glioma dataset revealed that patients with high B7-H3 expression presented with worse overall survival (OS) than those with low B7-H3 expression ( $n = 514$ ; Figure 1I). Together, these data suggested that B7-H3 promotes glioma growth and invasion, resulting in a poor prognosis for glioma patients.

## B7-H3 Regulated Tumor Progression Through Activation of the JAK2/STAT3 Signaling Pathway

Increasing evidence has indicated that B7-H3 can regulate tumor progression through JAK2/STAT3 signaling.<sup>24</sup> Therefore, we examined the expression of p-JAK2, total JAK2, p-STAT3, and total STAT3 in LN229-vector, LN229-B7-H3 OE, U87-vector, and U87-B7-H3 OE cells. The results showed that the levels of p-JAK2 and p-STAT3 were increased in glioma cells overexpressing B7-H3, indicating that the JAK2/STAT3 signaling pathway had been activated (Figure 2A). Previous reports indicated that IL-6 could activate JAK-STAT and inhibit SOCS-3 (suppressor of cytokine signaling 3) and SHP-1 (Src homology 2 [SH2]-containing phosphatase-1).<sup>16</sup> We therefore examined the expression of SOCS-3, SHP-1, and Src in LN229-vector, LN229-B7-H3 OE, U87-vector, and U87-B7-H3 OE cells.

We found that Src phosphorylation was enhanced, whereas the levels of p-SHP-1, total SHP-1, and SOCS-3 were reduced in glioma cells overexpressing B7-H3 (Figure 2B). These results suggested that B7-H3 induced Src activation and downregulated the levels of the negative regulators SOCS-3/SHP-1, thereby activating JAK2/STAT3 signaling. To further assess the role of JAK2/STAT3 signaling in B7-H3-induced glioma progression, we treated B7-H3-overexpressing glioma cells with FLN32, a JAK2/STAT3 inhibitor. Notably, the B7-H3-induced proliferation of glioma cells was delayed following FLN32 treatment (Figure 2C). Additionally, FLN32 treatment also suppressed the B7-H3-induced increase in colony formation, tumorigenesis, and invasion of glioma cells (Figure 2D–F), further indicating that B7-H3 induces the sustained growth and invasive capacity of glioma cells through the JAK2/STAT3 pathway. Consistent with this conclusion, increased levels of p-JAK2 and p-STAT3 were also observed in tissues from patients with malignant gliomas (Figure 2G).

## B7-H3 Facilitated Glioma Cell Invasion Through Slug-Induced EMT

The STAT3 signal can induce EMT through activation of the Slug and Snail (SNAI1) transcription factors, resulting in tumor cell invasion in several cancer types.<sup>25,26</sup> Based on these findings, we assessed the expression of the EMT markers E-cadherin and N-cadherin in glioma cells overexpressing B7-H3. We found that N-cadherin expression was increased, whereas that of E-cadherin was reduced, in B7-H3-overexpressing cells compared with control cells expressing the empty vector; however, blockade of the JAK2/STAT3 signal reversed these effects, indicating that B7-H3 facilitated EMT through JAK2/STAT3 signaling in glioma (Figure 3A). Slug expression was also upregulated in glioma cells overexpressing B7-H3 (Figure 3B). These results suggested that B7-H3 may be involved in EMT processes through Slug, a downstream target of JAK2/STAT3. To further assess the role of Slug in glioma invasion, we knocked down Slug in LN229-B7-H3 OE and U87-B7-H3 OE cells (Figure 3C). Intriguingly, we found that Slug knockdown suppressed B7-H3-induced EMT (Figure 3D) and glioma cell invasion (Figure 3E). Together, these results indicated that B7-H3 promotes EMT through the JAK2/STAT3/Slug signaling pathway. Increasing evidence has indicated that activation of the JAK/STAT3/Slug signal regulates EMT processes through expression of the matrix metalloproteinases MMP-2 and



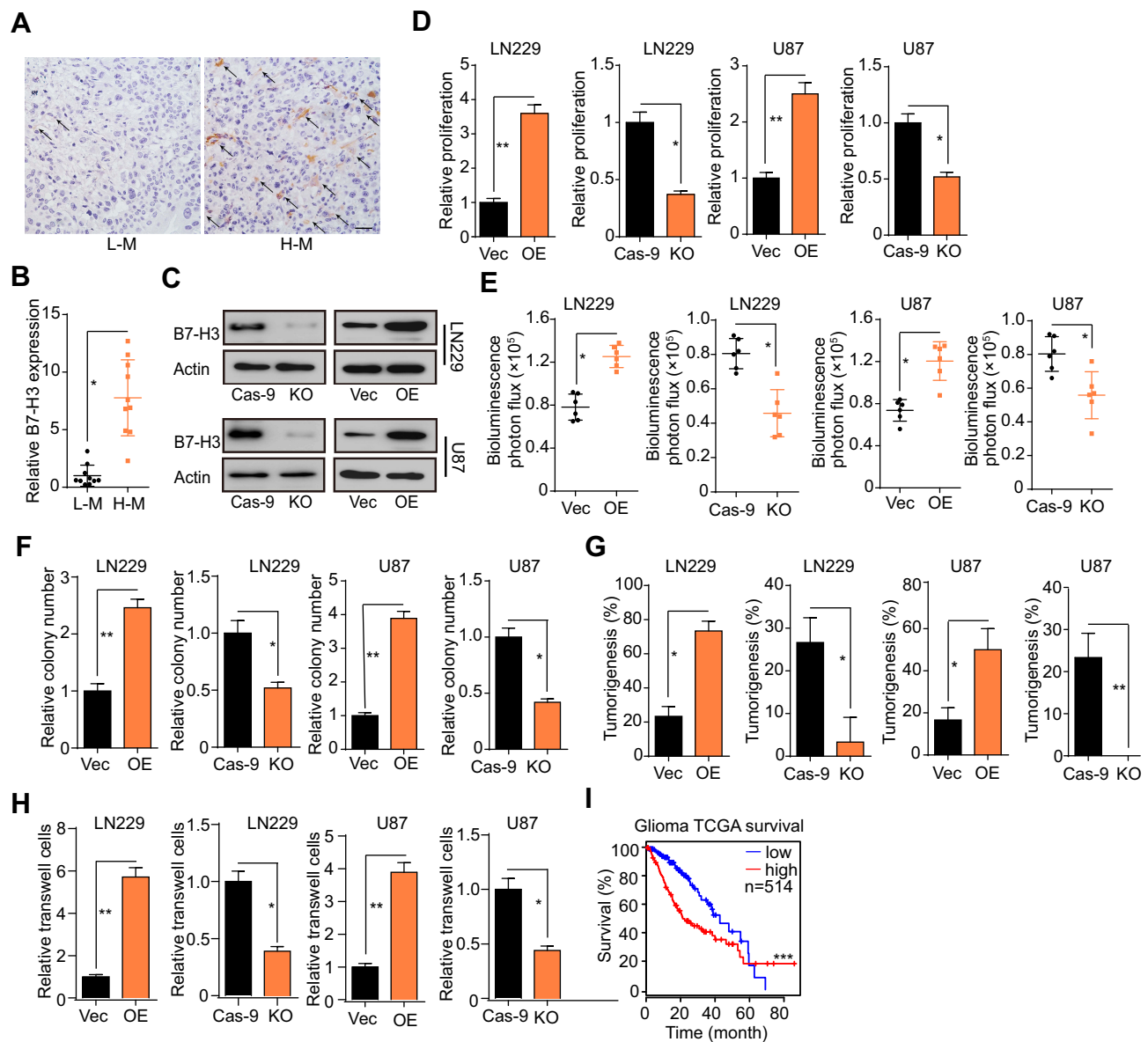


**Figure 1** B7-H3 facilitates glioma cell proliferation and invasion. **(A)** Immunohistochemistry for B7-H3 in high-grade malignancy (H-M) and low-grade malignancy (L-M) glioma tissues from patients. Scale bar, 50  $\mu$ m. **(B)** The relative expression levels of B7-H3 in H-M and L-M glioma tissues from patients ( $n = 10$ ). **(C)** Western blotting assay of B7-H3 expression in LN229-vector, LN229-B7-H3 OE, LN229-Cas9, and LN229-B7-H3 KO cells and U87-vector, U87-B7-H3-OE, U87-Cas9, and U87-B7-H3 KO cells. **(D)** CCK-8 assay for the relative proliferation rates of LN229-vector, LN229 B7-H3-OE, LN229-Cas9, and LN229-B7-H3 KO cells and U87-vector, U87 B7-H3-OE, U87-Cas9, and U87-B7-H3 KO cells. **(E)** Quantification of luciferase intensity in luciferase-labeled LN229 vector, LN229 B7-H3 OE, LN229 Cas9, and LN229 B7-H3 KO cell-bearing mice ( $1 \times 10^6$  cells,  $n = 6$ ) and U87 vector, U87 B7-H3 OE, U87 Cas9, and U87 B7-H3 KO cell-bearing mice ( $1 \times 10^6$  cells,  $n = 6$ ) on day 25 after xenograft. **(F)** Relative colony numbers of 500 LN229-vector, LN229-B7-H3 OE, LN229-Cas9, and LN229-B7-H3 KO cells and 500 U87-vector, U87-B7-H3 OE, U87-Cas9, and U87-B7-H3 KO cells. **(G)** Tumorigenesis in mice subcutaneously injected with  $5 \times 10^4$  LN229-vector, LN229-B7-H3 OE, LN229-Cas9, and LN229-B7-H3 KO cells ( $n = 10$ ) and  $5 \times 10^4$  U87-vector, U87-B7-H3 OE, U87-Cas9, and U87-B7-H3 KO cells ( $n = 10$ ) 30 days after xenograft. **(H)** Relative numbers of invasive LN229-vector, LN229-B7-H3 OE, LN229-Cas9, and LN229-B7-H3 KO cells ( $1 \times 10^4$ ) and U87-vector, U87-B7-H3 OE, U87-Cas9, and U87-B7-H3 KO cells ( $1 \times 10^4$ ) over 24 h. **(I)** Kaplan-Meier survival analysis of 514 glioma patients from TCGA; patients were divided into a high B7-H3 expression group ( $n = 257$ ) and a low B7-H3 expression group ( $n = 257$ ). The data are presented as means  $\pm$  SEM of at least three independent experiments. \* $p < 0.05$ , \*\* $p < 0.01$ , \*\*\* $p < 0.001$ .

**Abbreviation:** ns, not significant.

MMP-9. Accordingly, we found that the expression of MMP-2 and MMP-9 was increased in B7-H3-overexpressing glioma cells, whereas inhibition of the JAK2/STAT3 signal or Slug knockdown resulted in the suppression of MMP-2/-9 secretion (Figure 3F and G). In

line with previous results, treatment with MMP-2 or MMP-9 also efficiently facilitated LN229 and U87 cell invasion (Figure 3H). Importantly, we observed that the expression of MMP-2 and MMP-9 was upregulated in tumor tissues from H-M glioma patients compared with

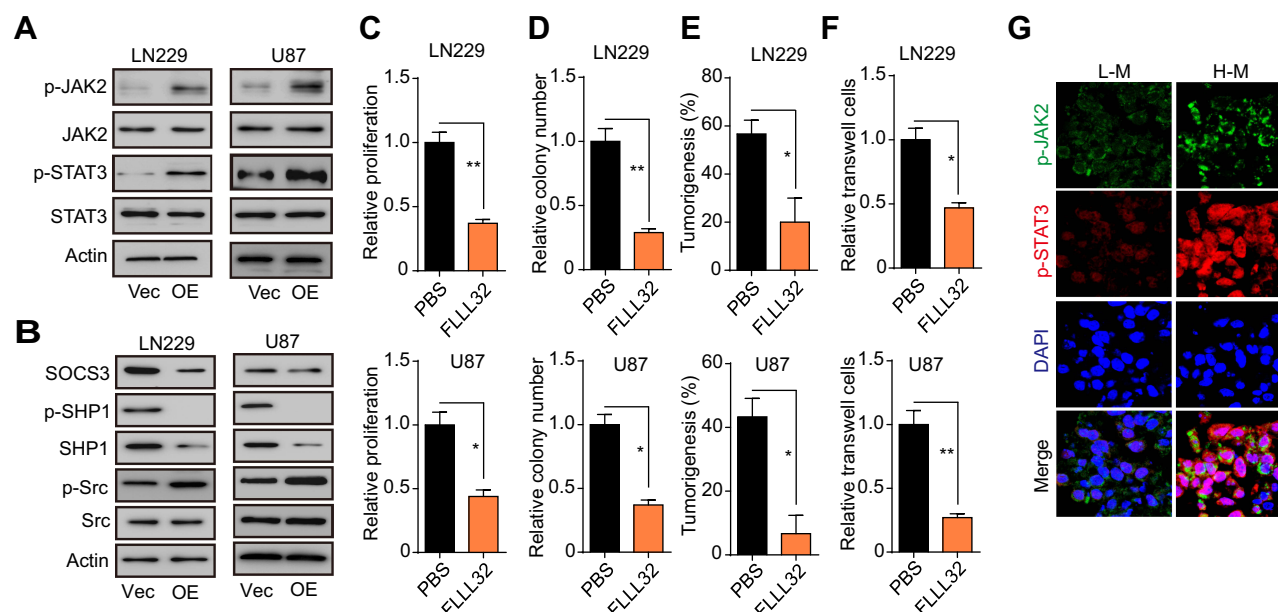


**Figure 2** B7-H3 promotes glioma growth and invasion through the JAK2/STAT3 signaling pathway. **(A)** Western blot analysis of p-JAK2, total JAK2, p-STAT3, and total STAT3 expression in LN229-vector, LN229-B7-H3 OE, U87-vector, and U87-B7-H3 OE cells. **(B)** Western blot analysis of SOCS-3, p-SHP1, total SHP1, p-Src, and total Src expression in LN229-vector, LN229-B7-H3 OE, U87-vector, and U87-B7-H3 OE cells. **(C)** Relative proliferation rates of LN229 B7-H3-OE cells and U87-B7-H3 OE cells treated with PBS or FLLL32 (1  $\mu$ M). **(D)** Relative colony numbers of LN229-B7-H3 OE cells and U87-B7-H3 OE cells treated with PBS or FLLL32 (1  $\mu$ M). **(E)** Tumorigenesis in mice subcutaneously injected with  $5 \times 10^4$  LN229-B7-H3 OE cells or U87-B7-H3 OE cells pretreated with PBS or FLLL32 (1  $\mu$ M) for 48 h. **(F)** Relative numbers of invasive LN229-B7-H3 OE cells or U87-B7-H3 OE cells (both  $1 \times 10^4$ ) treated with PBS or FLLL32 (1  $\mu$ M). **(G)** Immunofluorescence staining for p-JAK2 and p-STAT3 in tumor tissues from low-grade (L-M) or high-grade (H-M) glioma tissue from patients. Scale bar, 20  $\mu$ m. The data are presented as means  $\pm$  SEM of at least three independent experiments. \* $p < 0.05$ , \*\* $p < 0.01$ .

**Abbreviation:** ns, not significant.

those from L-M glioma patients (Figure 3I). Based on these results, we concluded that B7-H3 could induce glioma invasion through JAK2/STAT3/Slug/MMP-2/-9.

## Combination Treatment with TMZ and the STAT3 Inhibitor NAP Exerted Significant Anticancer Effects in Glioma

Several studies have indicated that activation of prosurvival signaling pathways, such as the PI3K/AKT and JAK/STAT signaling pathways, can induce sustained tumor growth and resistance to chemotherapy.<sup>27,28</sup> Therefore, we hypothesized that blocking the JAK2/STAT3 signal would strengthen the anticancer effects of chemotherapeutic agents and lead to improved clinical prognosis. NAP, a STAT3 inhibitor, can suppress tumor progression when administered orally, and is suitable for clinical glioma treatment.<sup>29,30</sup> Here, we used LN229-luc or LN229-B7-H3-luc cells to establish an orthotopic mouse glioma model, and used a live-imaging system to evaluate tumor growth. Next, NAP was orally administered in combination with TMZ for orthotopic glioma treatment. Intriguingly, combined TMZ and NAP treatment significantly suppressed glioma growth (Figure 4A and B)

and prolonged the survival of LN229-luc cell-bearing mice (Figure 4C). We also found that TMZ administration could not induce apoptosis in LN229-B7-H3-luc tumor cells in vivo, whereas treatment with NAP could efficiently inhibit the proliferation of LN229-B7-H3-luc cells and prolong the survival of xenografted mice (Figure 4D and E). These results indicated that NAP could efficiently suppress the sustained growth induced by STAT3 in glioma and improve the outcome in glioma treatment. We previously showed that B7-H3 expression can enhance glioma cell invasion. Consequently, we examined whether combined NAP and TMZ treatment could inhibit the invasive abilities of LN229-luc or LN229-B7-H3-luc cells. As expected, blockade of the STAT3 signal led to a significant delay in glioma cell invasion (Figure 4F and G). Together, these results suggested that blocking the STAT3 signal with NAP enhanced the anticancer effects of TMZ, thereby providing an innovative approach for the treatment of glioma.

## Discussion

It is well documented that B7-H3 is aberrantly expressed in several tumor types and is involved in early tumorigenesis or tumor development through immune-associated

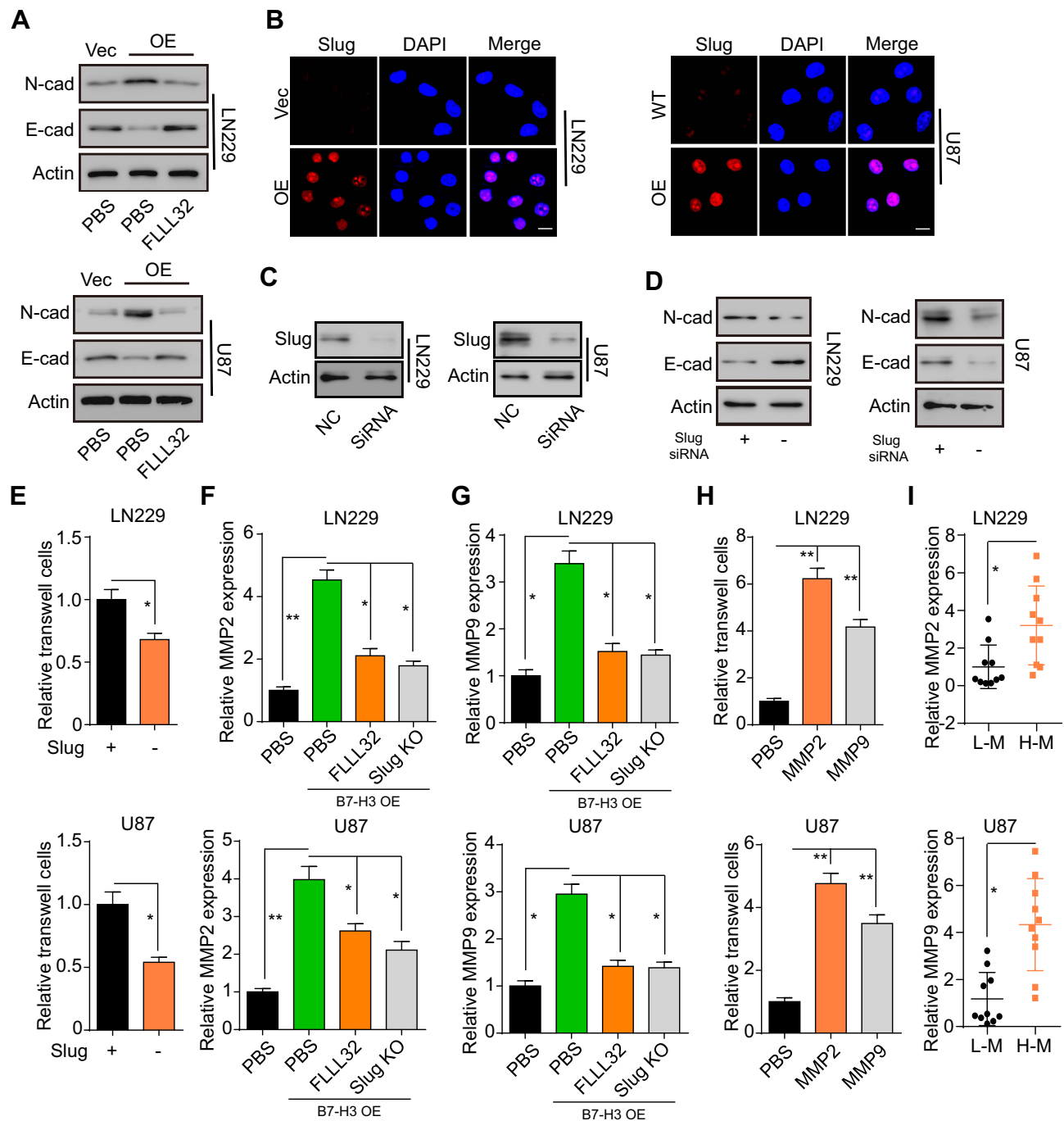


**Figure 3** B7-H3 induces EMT in glioma cells through upregulation of Slug. (A) Western blot analysis of N-cadherin and E-cadherin expression in LN229-vector, LN229 B7-H3-OE, U87-vector, and U87 B7-H3-OE cells treated with PBS or FLLL32 (1  $\mu$ M). (B) Immunofluorescence staining for Slug expression in LN229-vector, LN229 B7-H3-OE, U87-vector, and U87 B7-H3-OE cells. (C) Western blot analysis of Slug expression in LN229 and U87 cells treated or not with Slug siRNA. (D) Western blot analysis of N-cadherin and E-cadherin expression in Slug knockdown LN229-vector or LN229 B7-H3-OE cells and U87-vector or U87 B7-H3-OE cells. (E) Relative numbers of invasive LN229-B7-H3 OE or Slug knockdown LN229-B7-H3 OE cells ( $1 \times 10^4$ ), and U87-B7-H3 OE or Slug knockdown U87-B7-H3 OE cells ( $1 \times 10^4$ ). (F, G) ELISA for the relative expression of MMP-2 (F) and MMP-9 (G) in LN229-vector and LN229 B7-H3-OE cells treated with PBS or FLLL32 (1  $\mu$ M) or in Slug knockdown LN229 B7-H3-OE cells; and in U87-vector and U87 B7-H3-OE cells treated with PBS or FLLL32 (1  $\mu$ M) or in Slug knockdown U87 B7-H3-OE cells. (H) Relative numbers of invasive LN229 and U87 cells ( $1 \times 10^4$ ) treated with MMP-9 (100 ng/mL) or MMP-2 (100 ng/mL). (I) Relative expression of MMP-2 and MMP-9 in low-grade malignancy (L-M) or high-grade malignancy (H-M) tumor tissue from glioma patients. The data are presented as means  $\pm$  SEM of at least three independent experiments. \* $p < 0.05$ , \*\* $p < 0.01$ .

**Abbreviation:** ns, not significant.

pathways.<sup>14,16,31</sup> Existing evidence also indicates that higher B7-H3 expression is tightly correlated with poor prognosis in glioma patients.<sup>32</sup> In this study, we further

confirmed the role of B7-H3 in glioma development and invasion, which is consistent with previous reports for other tumor types.<sup>33</sup> We found that B7-H3 induced the

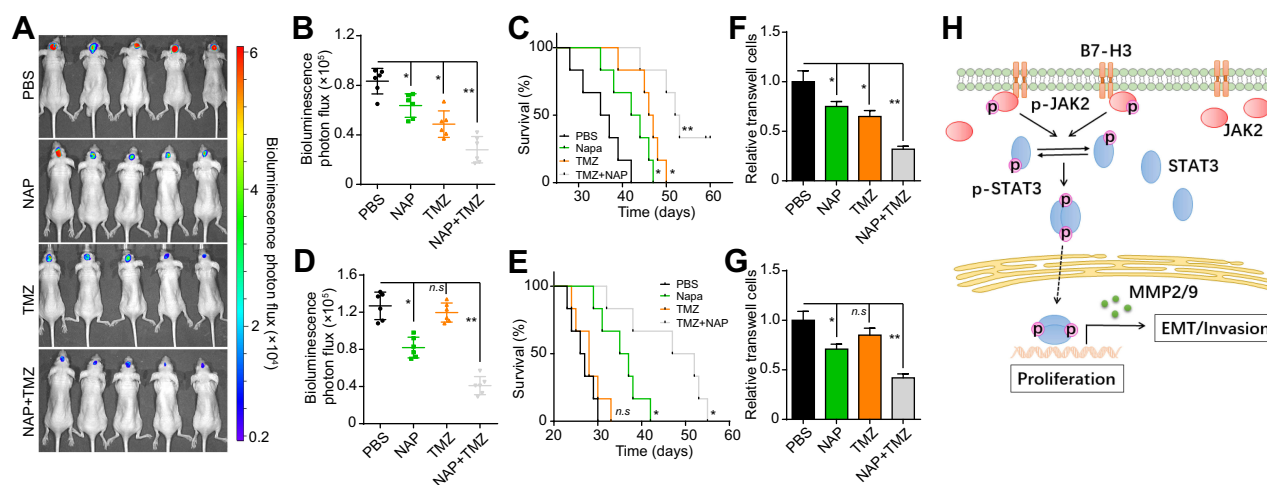


**Figure 4** A combination of temozolomide (TMZ) and nabucasin (NAP) efficiently suppressed glioma growth and invasion in vivo. **(A)** Representative bioluminescence image of mice intracranially injected with  $1 \times 10^6$  luciferase-labeled LN229 cells treated with PBS, NAP, TMZ, or NAP combined with TMZ. **(B)** Quantification of luciferase intensity in luciferase-labeled LN229 cell-bearing mice treated with PBS, NAP, TMZ, or NAP combined with TMZ. **(C)** Survival time of LN229 cell-bearing mice treated with PBS, NAP, TMZ, or NAP combined with TMZ. **(D)** Quantification of luciferase intensity in LN229-B7-H3 OE cell-bearing mice treated with PBS, NAP, TMZ, or NAP combined with TMZ. **(E)** Survival time of LN229-B7-H3 OE cell-bearing mice treated with PBS, NAP, TMZ, or NAP combined with TMZ. **(F, G)** Transwell assay for the invasion of LN229 **(F)** or LN229-B7-H3 OE cells **(G)** in culture medium with PBS, NAP (0.1  $\mu$ M), or TMZ (1  $\mu$ M). **(H)** Schematic overview of how B7-H3 regulates glioma growth and invasion through a JAK2/STAT3/Slug-dependent signaling pathway. The data are presented as means  $\pm$  SEM of three independent experiments. \* $p < 0.05$ , \*\* $p < 0.01$ . **Abbreviation:** ns, not significant.

activation of JAK2/STAT3 signaling through the upregulation of phosphorylated Src and inhibition of the negative regulators SHP-1 and SOCS-3. Moreover, JAK2/STAT3 signaling also induced the upregulation of the transcription factor Slug, thereby promoting EMT and MMP-2/-9 secretion in glioma cells. Blockade of JAK2/STAT3 signal significantly suppressed tumor growth and glioma cell invasion, which provides a new therapeutic target for the treatment of glioma (Figure 4H).

B7-H3, a member of the B7 family of immune-regulatory ligands, plays a crucial role in adaptive immune responses. Several studies have confirmed that B7-H3 is strictly correlated with tumor cell adhesion, migration, and invasion.<sup>14,31,34</sup> Overexpression of B7-H3 in lung adenocarcinoma patients is closely associated with lymph node invasion, distant metastasis, and disease stage. Downregulation of B7-H3 expression in human lung adenocarcinoma cells can suppress the proliferation, migration, and invasive capacity of cancer cells.<sup>35</sup> Additionally, higher expression of B7-H3 in cervical cancer tissue was reported to be significantly associated with the depth of cancer invasion and poor survival.<sup>15</sup> Silencing or overexpression of B7-H3 in cervical cancer cell lines showed that B7-H3 is involved in cell proliferation and apoptosis of various tumor cells.<sup>36</sup> However, the mechanism underlying the role of B7-H3 in tumor invasion remains unclear. In our study, we found that B7-H3 expression could induce

sustained glioma growth and enhance glioma cell invasion. Importantly, we revealed the potential molecular mechanism through which B7-H3 mediates these functional roles of glioma cells. The JAK2/STAT3 signaling pathway is important for tumor formation and transmission, and JAK2/STAT3 signaling is activated in various tumor types. We further showed that the JAK2/STAT3 pathway has a role in sustained glioma growth and that JAK2/STAT3 has potential as a novel therapeutic target for the treatment of glioma.

Cancer cell migration and tumor invasion can result in distant metastasis. The EMT, part of the transcriptional program that promotes invasive and distant metastatic phenotypes in cancer cells, can be considered as a state of cell de-differentiation. When undergoing EMT, tumor cells lose cellular polarity and contact with the surrounding extracellular matrix and exhibit increased motility and migratory ability, ultimately leading to widespread tumor invasion and metastatic lesions.<sup>37</sup> MMP-2 and MMP-9 are members of the MMP enzyme family believed to play important role in EMT and cancer metastasis.<sup>38</sup> Previous studies have demonstrated that B7-H3 enhances inflammatory responses and promotes MMP-9 expression in a pneumococcal meningitis animal model.<sup>39</sup> In osteosarcoma, B7-H3 also regulates cell migration and promotes tumor invasion through an MMP-2-associated signaling pathway.<sup>40</sup> Notably, enhanced expression of both B7-H3



and MMP-2/-9 has been detected in colorectal cancer patients, suggesting that B7-H3 has a role in MMP-2/-9-associated activity. Here, we further demonstrated that B7-H3 can induce EMT and MMP-2/-9 secretion through Slug, a downstream target of JAK2/STAT3, resulting in glioma cell invasion.

The results of this study enhance our knowledge of the role of B7-H3 in glioma growth and invasion. Ours is the first report to indicate that a correlation exists between B7-H3 and glioma, demonstrating that the elevated expression of B7-H3 can lead to malignant glioma development. We also identified the mechanism underlying the B7-H3-induced tumor progression, and showed for the first time that B7-H3 is involved in glioma growth and invasion through activation of JAK/STAT3/Slug signaling and regulation of EMT processes. Finally, we showed that combined NAP and TMZ treatment led to a significant improvement in glioma treatment outcome. Compared with previously reported molecular inhibitors, NAP can be orally administered, which is more suited to glioma treatment. Our results suggest that the level of B7-H3 expression in glioma tissue or serum may serve as a potential biomarker for glioma diagnosis or analysis of tumor progression.

## Conclusion

In summary, we showed that B7-H3 can upregulate JAK2/STAT3 signaling and facilitate EMT in glioma cells, thereby inducing glioma development. Blockade of STAT3 by NAP treatment efficiently inhibited glioma growth and invasion, which might serve as a novel therapeutic strategy for the treatment of glioma.

## Acknowledgments

This study was supported by the Project Program of the Neurosurgical Clinical Medical Research Center of Sichuan Province, the Science and Technology Support Project of Sichuan Province (2018JY0404), and the Science and Technology Foundation of Southwest Medical University (2017-ZRQN180, 2017-ZRQN-110).

## Author Contributions

Ligang Chen was involved in the study design. Chuanhong Zhong was a major contributor in writing the manuscript. Yitian Chen analyzed the patient data. Bei Tao conducted the in vitro and in vivo experiments. All authors approved the final manuscript. All authors contributed toward data

analysis, drafting and revising the paper and agree to be accountable for all aspects of the work.

## Disclosure

The authors report no conflicts of interest in this work.

## References

1. Lapointe S, Perry A, Butowski NA. Primary brain tumours in adults. *Lancet*. 2018;392(10145):432–446. doi:10.1016/S0140-6736(18)30990-5
2. Marshall GM, Carter DR, Cheung BB, et al. The prenatal origins of cancer. *Nat Rev Cancer*. 2014;14(4):277–289. doi:10.1038/nrc3679
3. Ostrom QT, Gittleman H, Fulop J, et al. CBTRUS statistical report: primary brain and central nervous system tumors diagnosed in the United States in 2008–2012. *Neuro-Oncology*. 2015;17(Suppl 4):iv1–iv62. doi:10.1093/neuonc/nov189
4. Miller AM, Shah RH, Pentsova EI, et al. Tracking tumour evolution in glioma through liquid biopsies of cerebrospinal fluid. *Nature*. 2019;565(7741):654–658. doi:10.1038/s41586-019-0882-3
5. Ma J, Benitez JA, Li J, et al. Inhibition of nuclear PTEN tyrosine phosphorylation enhances glioma radiation sensitivity through attenuated DNA repair. *Cancer Cell*. 2019;35(3):504–18.e7. doi:10.1016/j.ccell.2019.01.020
6. Lee YH, Martin-Orozco N, Zheng P, et al. Inhibition of the B7-H3 immune checkpoint limits tumor growth by enhancing cytotoxic lymphocyte function. *Cell Res*. 2017;27(8):1034–1045. doi:10.1038/cr.2017.90
7. Schildberg FA, Klein SR, Freeman GJ, Sharpe AH. Coinhibitory pathways in the B7-CD28 ligand-receptor family. *Immunity*. 2016;44(5):955–972. doi:10.1016/j.immuni.2016.05.002
8. Burvenich IJG, Parakh S, Lee FT, et al. Molecular imaging of T cell co-regulator factor B7-H3 with (89)Zr-DS-5573a. *Theranostics*. 2018;8(15):4199–4209. doi:10.7150/thno.25575
9. Benzon B, Zhao SG, Haffner MC, et al. Correlation of B7-H3 with androgen receptor, immune pathways and poor outcome in prostate cancer: an expression-based analysis. *Prostate Cancer Prostatic Dis*. 2017;20(1):28–35. doi:10.1038/pcan.2016.49
10. Mao Y, Chen L, Wang F, et al. Cancer cell-expressed B7-H3 regulates the differentiation of tumor-associated macrophages in human colorectal carcinoma. *Oncol Lett*. 2017;14(5):6177–6183. doi:10.3892/ol.2017.6935
11. Chen W, Liu P, Wang Y, et al. Characterization of a soluble B7-H3 (sB7-H3) spliced from the intron and analysis of sB7-H3 in the sera of patients with hepatocellular carcinoma. *PLoS One*. 2013;8(10):e76965. doi:10.1371/journal.pone.0076965
12. Bachawal SV, Jensen KC, Wilson KE, Tian L, Lutz AM, Willmann JK. Breast cancer detection by B7-H3-targeted ultrasound molecular imaging. *Cancer Res*. 2015;75(12):2501–2509. doi:10.1158/0008-5472.CAN-14-3361
13. Zhang S, Zhou C, Zhang D, Huang Z, Zhang G. The anti-apoptotic effect on cancer-associated fibroblasts of B7-H3 molecule enhancing the cell invasion and metastasis in renal cancer. *Onco Targets Ther*. 2019;12:4119–4127.
14. Seaman S, Zhu Z, Saha S, et al. Eradication of tumors through simultaneous ablation of CD27/B7-H3-positive tumor cells and tumor vasculature. *Cancer Cell*. 2017;31(4):501–15.e8. doi:10.1016/j.ccell.2017.03.005
15. Li Y, Zhang J, Han S, et al. B7-H3 promotes the proliferation, migration and invasiveness of cervical cancer cells and is an indicator of poor prognosis. *Oncol Rep*. 2017;38(2):1043–1050. doi:10.3892/or.2017.5730
16. Lin L, Cao L, Liu Y, et al. B7-H3 promotes multiple myeloma cell survival and proliferation by ROS-dependent activation of Src/STAT3 and c-Cbl-mediated degradation of SOCS3. *Leukemia*. 2019;33(6):1475–1486. doi:10.1038/s41375-018-0331-6

17. Wang T, Fahrman JF, Lee H, et al. JAK/STAT3-regulated fatty acid beta-oxidation is critical for breast cancer stem cell self-renewal and chemoresistance. *Cell Metab.* **2018**;27(1):136–50 e5. doi:10.1016/j.cmet.2017.11.001
18. Xu XF, Gao F, Wang JJ, et al. BMX-ARHGAP fusion protein maintains the tumorigenicity of gastric cancer stem cells by activating the JAK/STAT3 signaling pathway. *Cancer Cell Int.* **2019**;19:133. doi:10.1186/s12935-019-0847-5
19. Johnson DE, O'keefe RA, Grandis JR. Targeting the IL-6/JAK/STAT3 signalling axis in cancer. *Nat Rev Clin Oncol.* **2018**;15(4):234–248. doi:10.1038/nrclinonc.2018.8
20. Yang J, Xing H, Lu D, et al. Role of Jagged1/STAT3 signalling in platinum-resistant ovarian cancer. *J Cell Mol Med.* **2019**;23(6):4005–4018. doi:10.1111/jcmm.2019.23.issue-6
21. Wu X, Tao P, Zhou Q, et al. IL-6 secreted by cancer-associated fibroblasts promotes epithelial-mesenchymal transition and metastasis of gastric cancer via JAK2/STAT3 signaling pathway. *Oncotarget.* **2017**;8(13):20741–20750. doi:10.18632/oncotarget.15119
22. Lin L, Cao L, Liu Y, et al. B7-H3 promotes multiple myeloma cell survival and proliferation by ROS-dependent activation of Src/STAT3 and c-Cbl-mediated degradation of SOCS3. *Leukemia.* **2019**;33(6):1475–1486.
23. Flem-Karlsen K, Fodstad O, Tan M, Nunes-Xavier CE. B7-H3 in cancer - beyond immune regulation. *Trends Cancer.* **2018**;4(6):401–404. doi:10.1016/j.trecan.2018.03.010
24. Kang FB, Wang L, Jia HC, et al. B7-H3 promotes aggression and invasion of hepatocellular carcinoma by targeting epithelial-to-mesenchymal transition via JAK2/STAT3/Slug signaling pathway. *Cancer Cell Int.* **2015**;15:45. doi:10.1186/s12935-015-0195-z
25. Yao C, Su L, Shan J, et al. IGF/STAT3/NANOG/slug signaling axis simultaneously controls epithelial-mesenchymal transition and stemness maintenance in colorectal cancer. *Stem Cells.* **2016**;34(4):820–831. doi:10.1002/stem.v34.4
26. Kong G, Jiang Y, Sun X, et al. Irisin reverses the IL-6 induced epithelial-mesenchymal transition in osteosarcoma cell migration and invasion through the STAT3/Snail signaling pathway. *Oncol Rep.* **2017**;38(5):2647–2656. doi:10.3892/or.2017.5973
27. Blank CU, Haining WN, Held W, et al. Defining 'T cell exhaustion'. *Nat Rev Immunol.* **2019**;19(11):665–674. doi:10.1038/s41577-019-0221-9
28. Lui AJ, Geanes ES, Ogony J, et al. IFITM1 suppression blocks proliferation and invasion of aromatase inhibitor-resistant breast cancer in vivo by JAK/STAT-mediated induction of p21. *Cancer Lett.* **2017**;399:29–43. doi:10.1016/j.canlet.2017.04.005
29. Yan HHN, Siu HC, Law S, et al. A comprehensive human gastric cancer organoid biobank captures tumor subtype heterogeneity and enables therapeutic screening. *Cell Stem Cell.* **2018**;23(6):882–97. e11. doi:10.1016/j.stem.2018.09.016
30. Han D, Yu T, Dong N, Wang B, Sun F, Jiang D. Napabucasin, a novel STAT3 inhibitor suppresses proliferation, invasion and stemness of glioblastoma cells. *J Exp Clin Cancer Res.* **2019**;38(1):289. doi:10.1186/s13046-019-1289-6
31. Tekle C, Nygren MK, Chen YW, et al. B7-H3 contributes to the metastatic capacity of melanoma cells by modulation of known metastasis-associated genes. *Int J Cancer Manag.* **2012**;130(10):2282–2290. doi:10.1002/ijc.26238
32. Wang Z, Wang Z, Zhang C, et al. Genetic and clinical characterization of B7-H3 (CD276) expression and epigenetic regulation in diffuse brain glioma. *Cancer Sci.* **2018**;109(9):2697–2705. doi:10.1111/cas.13744
33. Lim S, Liu H, Madeira da Silva L, et al. Immunoregulatory protein B7-H3 reprograms glucose metabolism in cancer cells by ROS-mediated stabilization of HIF1alpha. *Cancer Res.* **2016**;76(8):2231–2242. doi:10.1158/0008-5472.CAN-15-1538
34. Li Y, Guo G, Song J, et al. B7-H3 promotes the migration and invasion of human bladder cancer cells via the PI3K/Akt/STAT3 signaling pathway. *J Cancer.* **2017**;8(5):816–824. doi:10.7150/jca.17759
35. Yu TT, Zhang T, Lu X, Wang RZ. B7-H3 promotes metastasis, proliferation, and epithelial-mesenchymal transition in lung adenocarcinoma. *Oncotargets Ther.* **2018**;11:4693–4700. doi:10.2147/OTT.S169811
36. Han S, Shi X, Liu L, et al. Roles of B7-H3 in cervical cancer and its prognostic value. *J Cancer.* **2018**;9(15):2612–2624. doi:10.7150/jca.24959
37. Yeung KT, Yang J. Epithelial-mesenchymal transition in tumor metastasis. *Mol Oncol.* **2017**;11(1):28–39. doi:10.1002/1878-0261.12017
38. Yang F, Yu N, Wang H, et al. Downregulated expression of hepatoma-derived growth factor inhibits migration and invasion of prostate cancer cells by suppressing epithelial-mesenchymal transition and MMP2, MMP9. *PLoS One.* **2018**;13(1):e0190725. doi:10.1371/journal.pone.0190725
39. Chen X, Bai Y, Cui W, et al. Effects of B7-H3 on the inflammatory response and expression of MMP-9 in mice with pneumococcal meningitis. *J Mol Neurosci.* **2013**;50(1):146–153. doi:10.1007/s12031-012-9885-3
40. Wang L, Zhang Q, Chen W, et al. B7-H3 is overexpressed in patients suffering osteosarcoma and associated with tumor aggressiveness and metastasis. *PLoS One.* **2013**;8(8):e70689. doi:10.1371/journal.pone.0070689

## OncoTargets and Therapy

### Publish your work in this journal

OncoTargets and Therapy is an international, peer-reviewed, open access journal focusing on the pathological basis of all cancers, potential targets for therapy and treatment protocols employed to improve the management of cancer patients. The journal also focuses on the impact of management programs and new therapeutic

agents and protocols on patient perspectives such as quality of life, adherence and satisfaction. The manuscript management system is completely online and includes a very quick and fair peer-review system, which is all easy to use. Visit <http://www.dovepress.com/testimonials.php> to read real quotes from published authors.

Submit your manuscript here: <https://www.dovepress.com/oncotargets-and-therapy-journal>

Dovepress